University of Huddersfield Repository

Ge, Q., Yap, Y.F., Zhang, M. and Chai, John

Modeling anisotropic diffusion using a departure from isotropy approach

Original Citation

Ge, Q., Yap, Y.F., Zhang, M. and Chai, John (2013) Modeling anisotropic diffusion using a departure from isotropy approach. Computers & Fluids, 86. pp. 298-309. ISSN 00457930

This version is available at http://eprints.hud.ac.uk/id/eprint/21752/

Modeling Anisotropic Diffusion Using A Departure From Isotropy Approach

Q. Ge[1], Y.F. Yap[1]*, M. Zhang[2] and J.C. Chai[1]

[1]Depart. of Mechanical Eng., Petroleum Institute, Abu Dhabi, UAE.

[2]School of Energy & Power Eng., Nanjing University of Science & Technology, Nanjing, P.R. China.

*Corresponding author:

Tel: +971 2 607 5175

Fax: +971 2 607 5200

Email address: yfatt@pi.ac.ae

Address:

The Petroleum Institute

Department of Mechanical Engineering

P.O. Box 2533, Abu Dhabi, UAE.

Abstract

There are a large number of finite volume solvers available for solution of *isotropic* diffusion equation. This article presents an approach of adapting these solvers to solve *anisotropic* diffusion equations. The formulation works by decomposing the diffusive flux into a component associated with isotropic diffusion and another component associated with *departure* from isotropic diffusion. This results in an *isotropic* diffusion equation with additional terms to account for the anisotropic effect. These additional terms are treated using a deferred correction approach and coupled via an iterative procedure. The presented approach is validated against various diffusion problems in anisotropic media with known analytical or numerical solutions. Although demonstrated for two-dimensional problems, extension of the present approach to three-dimensional problems is straight forward. Other than the finite volume method, this approach can be applied to any discretization method.

Keywords: Anisotropic diffusion, finite volume method

1 Introduction

Isotropic diffusion equation governs a very wide range of physical processes occurring in isotropic media, including heat, mass and momentum transfers. Most media encountered in physical and engineering applications are however anisotropic in nature. For these media, the directional dependence of their diffusion coefficients must be accounted for. This equation needs to be further generalized by introducing the generalized Fick's law [1-2] with an anisotropic diffusion coefficient, and thus forming the anisotropic diffusion equation with additional mixed derivative terms. These mixed derivative terms characterize the more complicated interactions in the physical process originated from the anisotropy of the media under investigation. Isotropic diffusion equation is therefore a very special limiting case of an anisotropic diffusion equation.

Anisotropic diffusion equation arises in very diverse physical processes. Diffusion of water vapours, organic vapours and gases in soil, diffusion of nutrients away from fertilizer granules towards plant roots in soil and diffusion of contaminants within subsurface geological formations are examples of solutal diffusion transport in porous media [3-5]. The structure of these naturally occurring porous media is highly irregular in terms of the pore distribution with respect to both size and shape. Given the anisotropy (and the heterogeneity) of the media, such diffusion processes can be appropriately modelled with an anisotropic diffusion equation. Besides, the generalized Darcy's law coupled with the continuity equation for modeling fluid flow in anisotropic heterogeneous porous media, e.g. subsurface geological formations, gives rise to a similar anisotropic diffusion equation in terms of

the fluid pressure [6-7]. Heat transfer in structural materials, e.g. wood and laminated metal sheets, and crystals is another flourishing field where anisotropic diffusion equation is generally applied [8-10]. Interestingly, in the recent years, anisotropic diffusion equation finds its application in the field of imaging, e.g. diffusion-tensor magnetic resonance imaging [11] and more generally PDE-based anisotropic diffusion filters [12-14].

From a historical point of view, solutions of isotropic diffusion equation were attempted much earlier than that of anisotropic diffusion equation. Isotropic diffusion equation has a lucidly simpler mathematical structure and therefore is more amenable to both analytical and numerical approaches. Some of these developed numerical approaches, e.g. based on the finite difference (FD), finite volume (FV), finite element (FE), boundary element (BE) methods and fast Poisson solver [15-19], are now well established and implemented routinely as standard solvers, at least for simple geometrical configurations. For more complicated geometrical configurations, numerical solution implemented on unstructured mesh is still being actively pursued for example in the recent work of [20]. Driven by the pressing needs of the above mentioned practical applications involving anisotropic media, these methods are then generalized to anisotropic diffusion equation. Such generalizations require careful consideration of the discretization procedure that gives proper discretization of the diffusion terms.

The applications of FD method for various anisotropic diffusion problems were made in [7, 21-22]. In [21], the coordinate system is realigned with the principal direction of the anisotropic diffusion coefficient so that the cross derivative terms vanish. This approach is however difficult to be generalized for heterogeneous media where the principal direction changes spatially. Of particular interest is the improvement made by the introduction of mimetic approach [23-24]. Mimetic approach incorporates the essential property of conservation during the discretization procedure and gives locally conservative discretization equations. The FV method was also extended and employed in the works of [25-27]. For FV method, an accurate approximation of the flux at the control volume face remains one of the challenges. Flux-continuity across the control volume faces has been given extra attention to produce locally conservative schemes [27-29]. Matrix- [30] and flux-splitting [31] approaches were formulated for the FV method on structured and unstructured mesh. These approaches employ a deferred correction approach so that the coefficient matrix and the flux vector retain similar forms as those resulted from simple diffusion problems. The FE method was employed in [32-33] with proper modifications in the treatment of the additional mixed derivative terms. One notable effort that increase the method's accuracy is incorporation of the adaptive mesh approach into the framework of a FE method where the underlying mesh adapts

dynamically during the solution process was developed [34]. This adaptive mesh approach although costly gives excellent results with much lesser numerical smearing for diffusion in highly anisotropic media. Extension and applications of the BE method in various problems involving conduction heat transfer, fluid flow in porous media and structural problem of an elliptical bar under torsion have been demonstrated in [35-36]. It should be mentioned that some of these extensions require intricate discretization procedure and therefore not straight forward to implement numerically.

Here in this article, an alternative approach that adapts the existing solvers for isotropic diffusion equation to solve anisotropic diffusion equation is presented. In this approach, the diffusive flux is decomposed into a component associated with isotropic diffusion and another component associated with *departure* from isotropic diffusion. This decomposition transforms an anisotropic diffusion equation into the form of an isotropic diffusion equation with additional terms to account for the anisotropic effect. These additional terms are treated using a deferred correction approach and coupled via an iterative procedure. The advantage of the decomposition approach proposed here is that it allows existing solvers for isotropic problems to be extended easily to anisotropic diffusion problems (at least for orthogonal coordinate systems). The main contribution of this proposed approach is the simplicity it offers in the implementation of such an extension. It just requires an additional subroutine be written to evaluate the departure from isotropic term and called from the original solver. No other modification on the original code of the solver is required.

It should be noted that different deferred correction approaches have been proposed for the solution of anisotropic diffusion problems. In the flux-splitting approach at the flux level [30-31], the flux is split into the form of a leading two-point flux and additional cross-diffusion terms. The leading two-point flux term is approximated implicitly but the remainder flux term is treated explicitly and coupled iteratively. With this, the standard five-point (seven-point) stencil is preserved for two-dimensional (three-dimensional) problems. For flux-splitting at the matrix level [30-31], the coefficient matrix in the system of linear equations is effectively decomposed into a penta-diagonal matrix and a residual matrix. The penta-diagonal matrix is in the similar form that would be obtained by discretizing a simple diffusion equation. In the work of [25], only the cross diffusion terms are approximated explicitly via a deferred correction approach and coupled iteratively. Adaptation of these approaches into existing solvers for isotropic diffusion problems requires more modifications on the original code for the case where the diagonal components of the diffusion coefficient are different.

The remaining of the article is separated into five sections. A description of the problem is given in Section 2. Section 3 is the core of the article where the reformulation of the anisotropic diffusion equation is presented. The numerical solution procedure, including discretization, implementation of boundary conditions and convergence criterion, is discussed in Section 4. Validations of the present approach against seven different problems are given in Section 5. Finally, the article concludes with a few remarks in Section 6.

2 Problem Description

The domain of interest Ω, shown in Fig. 1, consists of an anisotropic medium. The steady-state diffusion transport of a quantity $\phi(\vec{x})$ within Ω is governed by the conservation equation

$$-\nabla \bullet \vec{q}(\vec{x}) + S(\vec{x}) = 0 \quad , \forall \vec{x} \in \Omega \tag{1}$$

where $\vec{q}(\vec{x})$ and $S(\vec{x})$ are the diffusion flux and the volumetric source/sink respectively. When $\vec{q}(\vec{x})$ is described by the generalized Fick's law, the anisotropic diffusion flux is as

$$\vec{q}(\vec{x}) = -\overline{\overline{\Gamma}}(\vec{x}) \bullet \nabla \phi(\vec{x}) \tag{2}$$

where $\overline{\overline{\Gamma}}(\vec{x})$ is the anisotropic diffusion coefficient, a second order tensor characterizing the anisotropy of the medium. Constrained by the Second Law of Thermodynamics, $\overline{\overline{\Gamma}}(\vec{x})$ is positive definite [42]. Substitution of Eq. (2) into Eq. (1) gives a second order elliptic *anisotropic* diffusion equation of the form

$$\nabla \bullet \left(\overline{\overline{\Gamma}}(\vec{x}) \bullet \nabla \phi(\vec{x}) \right) + S(\vec{x}) = 0 \quad , \forall \vec{x} \in \Omega \tag{3}$$

Equation (3) is subjected to the following mixed boundary condition, i.e. a combination of a prescribed $\phi^P(\vec{x})$ and a prescribed flux $q_n^P(\vec{x})$.

$$\phi(\vec{x}) = \phi^P(\vec{x}), \quad \forall \vec{x} \in \partial\Omega^\phi \tag{4a}$$

$$\vec{q}(\vec{x}) \bullet \vec{n}(\vec{x}) = q_n^P(\vec{x}), \quad \forall \vec{x} \in \partial\Omega^q \tag{4b}$$

where

$\partial\Omega^\phi \cup \partial\Omega^q = \partial\Omega$, $\partial\Omega^\phi \cap \partial\Omega^q = \varnothing$ and $\partial\Omega^\phi \neq \varnothing$. $\vec{n}$ is the unit normal vector pointing out of Ω. Dirichlet boundary condition is the limiting case of Eq. (4) when $\partial\Omega^q = \varnothing$. This article focuses on adapting solvers for *isotropic* diffusion equation to solve *anisotropic* diffusion equation (Eq. 3) subjected to the boundary condition of Eq. (4).
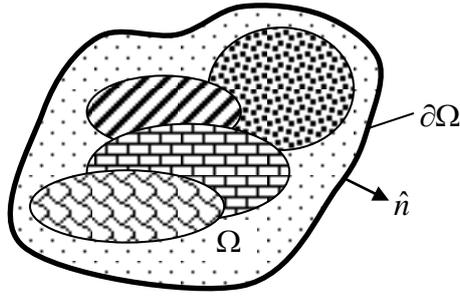
Figure 1: Domain of interest for an anisotropic diffusion problem.

3 Mathematical Formulation

Equation (3) can be reformulated into an *isotropic* diffusion equation. For this purpose, the anisotropic diffusion coefficient is decomposed as

$$\overline{\overline{\Gamma}}(\vec{x}) = \Gamma_{\max}(\vec{x})\overline{\overline{I}} + \overline{\overline{\Gamma_D}}(\vec{x}) \tag{5}$$

where

$$\Gamma_{\max}(\vec{x}) = \max\left\langle \Gamma_{xx}(\vec{x}), \Gamma_{yy}(\vec{x}), \Gamma_{zz}(\vec{x}) \right\rangle \tag{6a}$$

$$\overline{\overline{\Gamma_D}}(\vec{x}) = \begin{bmatrix} \Gamma_{xx}(\vec{x}) - \Gamma_{\max}(\vec{x}) & \Gamma_{xy}(\vec{x}) & \Gamma_{xz}(\vec{x}) \\ \Gamma_{yx}(\vec{x}) & \Gamma_{yy}(\vec{x}) - \Gamma_{\max}(\vec{x}) & \Gamma_{yz}(\vec{x}) \\ \Gamma_{zx}(\vec{x}) & \Gamma_{zy}(\vec{x}) & \Gamma_{zz}(\vec{x}) - \Gamma_{\max}(\vec{x}) \end{bmatrix} \tag{6b}$$

The operator $\max\langle a,b,c \rangle$ returns the largest of a, b and c. It was suggested by one of the reviewers of this article that for a symmetric Γ, $\Gamma_{\max}$ can also be set to the maximum of the eigenvalue so that the decomposition would be frame-independent. With this, $\vec{q}(\vec{x})$ can be written as

$$\vec{q}(\vec{x}) = \vec{q}_{\max}(\vec{x}) + \vec{q}_D(\vec{x}) \tag{7}$$

where

$$\vec{q}_{\max}(\vec{x}) = -\Gamma_{\max}(\vec{x})\nabla\phi(\vec{x}) \tag{8a}$$

$$\vec{q}_D(\vec{x}) = -\overline{\overline{\Gamma_D}}(\vec{x}) \bullet \nabla\phi(\vec{x}) \tag{8b}$$

Upon substitution of Eqs. (7) and (8) into to Eq. (1), Eq. (1) can now be expressed as

$$\nabla \bullet \left(\Gamma_{\max}(\vec{x})\nabla\phi(\vec{x}) \right) + S_D(\vec{x}) + S(\vec{x}) = 0 \quad , \forall \vec{x} \in \Omega \tag{9}$$

where

$$S_D(\vec{x}) = \nabla \bullet \left(\overline{\overline{\Gamma_D}}(\vec{x}) \bullet \nabla\phi(\vec{x}) \right) \quad , \forall \vec{x} \in \Omega \tag{10}$$

Equation (9) is the familiar *isotropic* diffusion equation. The first term on the left-side (LS) is referred to as the isotropic term as it captures diffusion in an isotropic medium of diffusion

6

coefficient $\Gamma_{max}(\vec{x})$. The additional source term $S_D(\vec{x})$ accounts for the effects due to the anisotropy of the medium. $S_D(\vec{x})$ is therefore referred as *departure* from isotropic term. The treatment of $S_D(\vec{x})$ will be further discussed in the next section. Essentially, the *anisotropic* diffusion equation (Eq. 3) is now in the form of an *isotropic* diffusion equation (Eq. 9). By incorporating the additional source term $S_D(\vec{x})$, a standard solver for *isotropic* diffusion equation can now be employed to solve Eq. (9).

4 Solution Procedure

4.1 Discretization

The finite volume method [17, 37] is employed to numerically solve Eq. (9) in two dimensions on a Cartesian mesh. Extension of the presented approach to three dimensions is straight forward. The physical domain is first partitioned into a number of non-overlapping control volumes (CVs) as shown in Fig. 2. A node is located at the centre of every CV. There are two types of CVs, i.e. internal CVs (e.g. CV P) and boundary CVs (e.g. CV P_B). For the internal CV P, the neighbouring nodes are labeled as W, E, N and S. It has four boundaries, denoted by e, w, n and s (with area of A_e, A_w, A_n and A_s respectively). The four corners of the CV P are denoted ne, nw, se and sw. The volume of the CV P is denoted as ΔV_P. ϕ, Γ_{max} and all the components of $\overline{\overline{\Gamma}}$ are stored at the nodes. For ease of reference and without the loss of generality, the dependence of the variables on $\vec{x}$ is implied implicitly and will therefore be dropped henceforth. Integration of Eq. (9) over the CV P gives

$$\oiiint_{\Delta V_P} \nabla \bullet (\Gamma_{max} \nabla \phi) dV + \oiiint_{\Delta V_P} S_D dV + \oiiint_{\Delta V_P} S dV = 0 \tag{11}$$

Employing the Gauss' divergence theorem, the volume integrations can be converted into surface integrations as

$$\oiint_{\Delta A_P} (\Gamma_{max} \nabla \phi) \bullet d\vec{A} + \oiint_{\Delta A_P} \left(\overline{\overline{\Gamma_D}} \bullet \nabla \phi \right) \bullet d\vec{A} + \oiiint_{\Delta V_P} S dV = 0 \tag{12}$$

The conversion of the 2nd term on the LS of Eq. (11) into a surface integration is important to ensure flux consistency in the discrezation equation. The terms in Eq. (12) can be approximated numerically as

$$\oiint_{\Delta A_P} (\Gamma_{max} \nabla \phi) \bullet d\vec{A}$$

$$= \left[\Gamma_{max} \frac{\partial \phi}{\partial x} \right]_e^m A_e - \left[\Gamma_{max} \frac{\partial \phi}{\partial x} \right]_w^m A_w + \left[\Gamma_{max} \frac{\partial \phi}{\partial y} \right]_n^m A_n - \left[\Gamma_{max} \frac{\partial \phi}{\partial y} \right]_s^m A_s \tag{13a}$$

$$\oiint_{\Delta A_P} \left(\overline{\overline{\Gamma_D}} \bullet \nabla \phi \right) \bullet d\vec{A}$$

$$= \left[\Gamma_{xy} \frac{\partial \phi}{\partial y} + \left(\Gamma_{xx} - \Gamma_{\max} \right) \frac{\partial \phi}{\partial x} \right]_e^{m-1} A_e - \left[\Gamma_{xy} \frac{\partial \phi}{\partial y} + \left(\Gamma_{xx} - \Gamma_{\max} \right) \frac{\partial \phi}{\partial x} \right]_w^{m-1} A_w$$

$$+ \left[\Gamma_{yx} \frac{\partial \phi}{\partial x} + \left(\Gamma_{yy} - \Gamma_{\max} \right) \frac{\partial \phi}{\partial y} \right]_n^{m-1} A_n - \left[\Gamma_{yx} \frac{\partial \phi}{\partial x} + \left(\Gamma_{yy} - \Gamma_{\max} \right) \frac{\partial \phi}{\partial y} \right]_s^{m-1} A_s \tag{13b}$$

$$\oiiint_{\Delta V_P} S dV = S_{ave}^{m-1} \Delta V_P \tag{13c}$$

The superscript m refers to quantities of the m iteration, i.e. the current iteration. Note that Eq. (13b) is calculated using the existing values of ϕ from the known $m-1$ iteration, i.e. previous iteration. By doing so, it becomes a 'known' source term. With this treatment, the discretization equation for Eq. (9) becomes that of an *isotropic* diffusion equation with 'known' source terms accounting for the anisotropy of the medium. A standard solver for *isotropic* diffusion equation can therefore be modified easily to solve Eq. (9). In Eqs. (13a) and (13b), $\left.\frac{\partial \phi}{\partial x}\right|_e$, $\left.\frac{\partial \phi}{\partial x}\right|_w$, $\left.\frac{\partial \phi}{\partial y}\right|_n$ and $\left.\frac{\partial \phi}{\partial y}\right|_s$ are approximated with central differences, assuming a linear variation of ϕ between two adjacent CVs. $\Gamma_{\max}$ and all the components of $\overline{\overline{\Gamma_D}}$ at the interface e, w, n and s are calculated via a harmonic mean for its superiority of maintaining the normal flux continuity. With these approximations, Eq. (12) becomes

$$a_P \phi_P^m = a_E \phi_E^m + a_W \phi_W^m + a_N \phi_N^m + a_S \phi_S^m + S_{ave}^{m-1} \Delta V_P + S_{dep}^{m-1} \tag{14}$$

where

$$a_E = \frac{\Gamma_{\max,e} A_e}{\delta x_{PE}} \tag{15a}$$

$$a_W = \frac{\Gamma_{\max,w} A_w}{\delta x_{PW}} \tag{15b}$$

$$a_N = \frac{\Gamma_{\max,n} A_n}{\delta y_{PN}} \tag{15c}$$

$$a_S = \frac{\Gamma_{\max,s} A_s}{\delta y_{PS}} \tag{15d}$$

$$a_P = a_E + a_W + a_N + a_S \tag{15e}$$

$$S_{dep}^{m-1} = +\Gamma_{xy,e}A_e \frac{\phi_{ne}^{m-1} - \phi_{se}^{m-1}}{\delta y} + \left(\Gamma_{xx} - \Gamma_{max}\right)_e A_e \frac{\phi_E^{m-1} - \phi_P^{m-1}}{\delta x_{PE}}$$

$$+ \Gamma_{xy,w}A_w \frac{\phi_{nw}^{m-1} - \phi_{sw}^{m-1}}{\delta y} + \left(\Gamma_{xx} - \Gamma_{max}\right)_w A_w \frac{\phi_P^{m-1} - \phi_W^{m-1}}{\delta x_{PE}}$$

$$+ \Gamma_{yx,n}A_n \frac{\phi_{ne}^{m-1} - \phi_{nw}^{m-1}}{\delta x} + \left(\Gamma_{yy} - \Gamma_{max}\right)_n A_n \frac{\phi_N^{m-1} - \phi_P^{m-1}}{\delta y_{PN}}$$

$$+ \Gamma_{yx,s}A_s \frac{\phi_{se}^{m-1} - \phi_{sw}^{m-1}}{\delta x} + \left(\Gamma_{yy} - \Gamma_{max}\right)_s A_s \frac{\phi_P^{m-1} - \phi_S^{m-1}}{\delta y_{PS}}$$

(15f)

In the evaluation of Eq. (15f), the values of ϕ_{ne}, ϕ_{nw}, ϕ_{se}, ϕ_{sw} are interpolated linearly from ϕ of the neighbouring nodes.
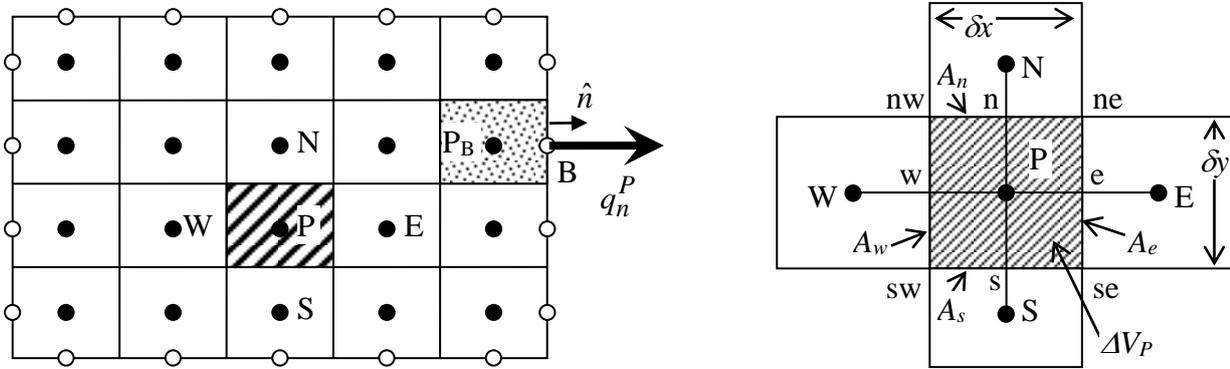
Figure 2: Partition of the domain of interest into non-overlapping control volumes.

4.2 Implementation of Boundary Conditions

The implementation of both a prescribed value ϕ^P and a prescribed flux q_n^P at the boundary are discussed here. For a prescribed ϕ^P, the imposition of Eq. (4a) is straight forward. ϕ at the boundary nodes, i.e. the hollow nodes in Fig. 2, is set to the prescribed ϕ^P. Of particular important is the imposition of a prescribed flux q_n^P, i.e. Eq. (4b). To implement this condition, the prescribed diffusion flux *out* of the domain at the boundary q_n^P is brought into the adjacent boundary CVs as a volumetric sink and the diffusion flux at the corresponding boundary is set to zero. Note that for flux of ϕ diffuses out of the domain, $q_n^P > 0$. For example, an additional sink term given by

$$S_{extra} = -\frac{q_n^P A_B}{\Delta V_{P_B}}$$

(16)

is added into the boundary CV P_B shown in Fig. 2. With this sink term added to account for the amount of ϕ diffuses out of the domain, the flux at the boundary can now be set zero, i.e.

$$\vec{q}(\vec{x}_B) \bullet \vec{n}(\vec{x}_B) = 0 \tag{17}$$

This can be achieved numerically by setting the associated diffusion coefficients in the discretization equation (Eqs. 13a and 13b) to zero, i.e.

$$\Gamma_{xx}\big|_e = \Gamma_{xy}\big|_e = \Gamma_{max}\big|_e = 0 \tag{18}$$

4.3 Solution Algorithm

The overall solution procedure can be summarized as follows:

(1) Specify Γ_{max} and $\overline{\overline{\Gamma_D}}$ in Eqs. (6).

(2) Calculate the volumetric source/sink $S(\vec{x})$ in Eq. (9).

(3) Calculate S_D from Eq. (10).

(4) Solve Eq. (9) for ϕ.

(5) Repeat steps (2) to (4) until the solution converges.

4.4 Convergence Criterion and Error Calculations

Application of the discretization equation (Eq. 14) to every CV gives a system of linear equation with penta-diagonal coefficient matrix. This system of linear equation is solved iteratively using the Thomas algorithm sweeping alternatively in the $x-$ and $y-$direction. No special initial guess is employed, i.e. $\phi_{i,j} = 0$. For convergence, the relative changes in ϕ between to successive iterations is monitored. The solution is assumed converged when $\|e\|_\infty < 10^{-8}$ where

$$\|e\|_\infty = \max_{\substack{i=1,..,M \\ j=1,...,N}} \left|1 - \phi_{i,j}^{m+1} / \phi_{i,j}^{m}\right| \tag{19}$$

For the cases considered in this article, a uniform mesh is employed. Mesh refinement is performed with a refinement ratio of $h = \dfrac{\Delta x}{\Delta x_0}$ where Δx_0 is the coarsest mesh. Error of the present solution will be reported in terms of maximum and root mean square norms discretely defined respectively as

$$\|E\|_\infty = \max_{\substack{i=1,..,M \\ j=1,...,N}} \left|\phi_{i,j}^{exact} - \phi_{i,j}^{num}\right| \tag{20}$$

$$\|E\|_2 = \sqrt[2]{\sum_{i=1,j=1}^{M,N} \left|\phi_{i,j}^{exact} - \phi_{i,j}^{num}\right|^2 \Delta V_{i,j}} \tag{21}$$

10

The order of accuracy is then *estimated* from the slope of the graph $\log\|E\|_2$ vs. $\log(h)$ fitted using the least square method.

5 Results and Discussions

The present approach is validated against known solutions for diffusion in various media subjected to either the limiting case of Dirichlet boundary condition or the more general mixed boundary condition. The first three validation exercises concern diffusion in heterogeneous anisotropic media with various forms of diffusion coefficients. The exact solutions for these cases were setup using the method of manufactured solution [38]. Two additional cases of diffusion in anisotropic media with discontinuous diffusion coefficient are then considered. This is followed finally by two applications of the presented approach for heat conduction in anisotropic medium with internal heat generation and flow in multi-layered anisotropic porous medium.

5.1 Diffusion in a heterogeneous anisotropic medium with a linear variable diffusion coefficient

The validation exercise starts with a medium with a simple linear diffusion coefficient. The domain of interest is a unit square of $\Omega = (0,1)^2$. The diffusion coefficient varies linearly in the domain as

$$\overline{\overline{\Gamma}} = \begin{bmatrix} 1+x+y & 0.5+y \\ 0.5+y & 1+2x+y \end{bmatrix} \tag{22}$$

Within the domain of interest, there is a non-zero variable source term given by

$$S = -(3+x+y)e^x - \cos y + (1+2x+y)\sin y \tag{23}$$

With these, it can be verified easily that the exact solution is given by

$$\phi = e^x + \sin y \tag{24}$$

Two tests of which the enforced boundary conditions are different will be considered. In the first test, the domain is subjected to the following Dirichlet boundary condition.

$$\phi^P(x,0) = e^x, \quad 0 \le x \le 1 \tag{25a}$$

$$\phi^P(x,1) = e^x + \sin 1, \quad 0 \le x \le 1 \tag{25b}$$

$$\phi^P(0,y) = 1 + \sin y, \quad 0 \le y \le 1 \tag{25c}$$

$$\phi^P(1,y) = e + \sin y, \quad 0 \le y \le 1 \tag{25d}$$

The second test, proposed in [39], subjects the domain to a mixed boundary condition of Eq. (26). While a prescribed ϕ^P is applied at the lower and upper boundaries, a prescribed flux q_n^P is enforced at both the left and right boundaries of the domain.

11

$$\phi^P(x,0) = e^x, \quad 0 \le x \le 1 \tag{26a}$$

$$\phi^P(x,1) = e^x + \sin 1, \quad 0 \le x \le 1 \tag{26b}$$

$$q_n^P(0,y) = +\left[1 + y + (0.5 + y)\cos y\right], \quad 0 \le y \le 1 \tag{26c}$$

$$q_n^P(1,y) = -\left[(2 + y)e + (0.5 + y)\cos y\right], \quad 0 \le y \le 1 \tag{26d}$$

Given the smooth nature of the solution, it is expected that most, if not all, of the essential features of the solutions can be well captured by a relatively coarse mesh. Mesh independent solutions were indeed obtained on the coarsest mesh of 25×25 CVs using the present approach for both boundary conditions. These solutions are presented together with the exact solution in Fig. 3. The present solutions agree well with the exact solution. The errors are plotted in Fig. 4. Both $\|E\|_\infty$ and $\|E\|_2$ decreases as the mesh is refined. Estimated from the slope of the graphs, the order of accuracy for the case of Dirichlet and mixed boundary conditions are respectively 1.7442 and 2.0816.

(a)　　　　　　　　　　　　　　　　　(b)
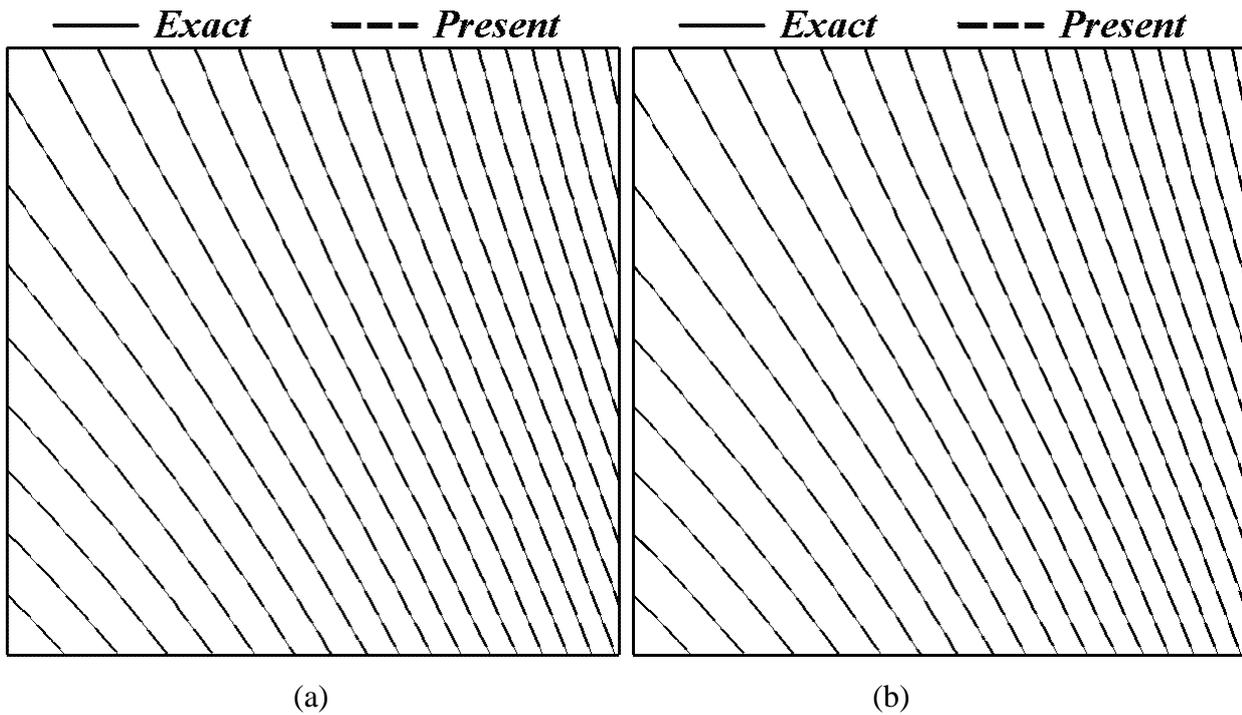
Figure 3: Solutions for diffusion in a medium with a linear variable diffusion coefficient subjected to (a) Dirichlet boundary condition and (b) mixed boundary condition.
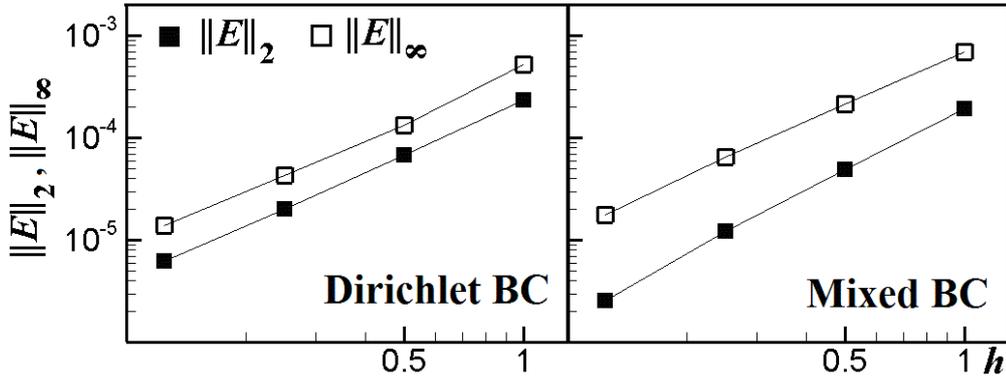
Figure 4: Errors for the case of diffusion in a medium with a linear variable diffusion coefficient.

5.2 Diffusion in a heterogeneous anisotropic medium with a non-linear variable diffusion coefficient

This exercise demonstrates the capability of the present approach in handling a more general form of the diffusion coefficient. Diffusion in again a unit square is considered for a non-linear variable diffusion coefficient of the form

$$\overline{\overline{\Gamma}} = \begin{bmatrix} \varepsilon x^2 + y^2 & -(1-\varepsilon)xy \\ -(1-\varepsilon)xy & x^2 + \varepsilon y^2 \end{bmatrix} \tag{27}$$

where ε characterizes the degree of anisotropy in the medium [40]. For $\varepsilon = 1$, the diffusion coefficient reduces to that of an isotropic medium. There is a non-zero variable source term in Ω given by

$$S = -(15\varepsilon - 7)x^2 y - (8\varepsilon + 4)x^2 - (24\varepsilon - 4)y^2 - 2y^3 \tag{28}$$

This problem has an exact solution in the form of

$$\phi = 1 + x^2 y + x^2 + 3y^2 \tag{29}$$

Note that the exact solution is independent of ε. The following mixed boundary condition of Eq. (27) is imposed on the boundary of the domain.

$$q_n^P(x,0) = x^4, \ 0 \le x \le 1 \tag{30a}$$

$$\phi^P(x,1) = 2x^2 + 3, \ 0 \le x \le 1 \tag{30b}$$

$$q_n^P(0,y) = 0, \ 0 \le y \le 1 \tag{30c}$$

$$q_n^P(1,y) = -(\varepsilon + y^2)(2y + 2) + (1-\varepsilon)(y + 6y^2), \ 0 \le y \le 1 \tag{30d}$$

For the case of $\varepsilon = 0.5$, mesh independent solution obtained on a coarsest mesh of 25×25 CVs is shown in Fig. 5a. For comparison purpose, the exact solution is superimposed. The present solution agrees well with the exact solution. Although not shown here, similar agreement is achieved where

the boundary is subjected to a Dirichlet boundary condition. The order of accuracy estimated from Fig. 6 is 1.7567.

The degree of anisotropy in the medium increases when ε is decreasing. For $\varepsilon \ll 1$, the medium is highly anisotropic. Either a very fine mesh or a multi-scale approach for example in [32] is then required to resolve the fine anisotropic features of the medium. For demonstration, the case of $\varepsilon = 0.01$ is now considered using the present approach. The solution on a mesh of $400 \times 400\,\text{CVs}$, much finer than the case of $\varepsilon = 0.5$, is plotted in Fig. 5b. Agreement with the superimposed exact solution is good. The order of accuracy is estimated to be 1.6962 surprisingly close to than that for the case of $\varepsilon = 0.5$.

(a)   (b)
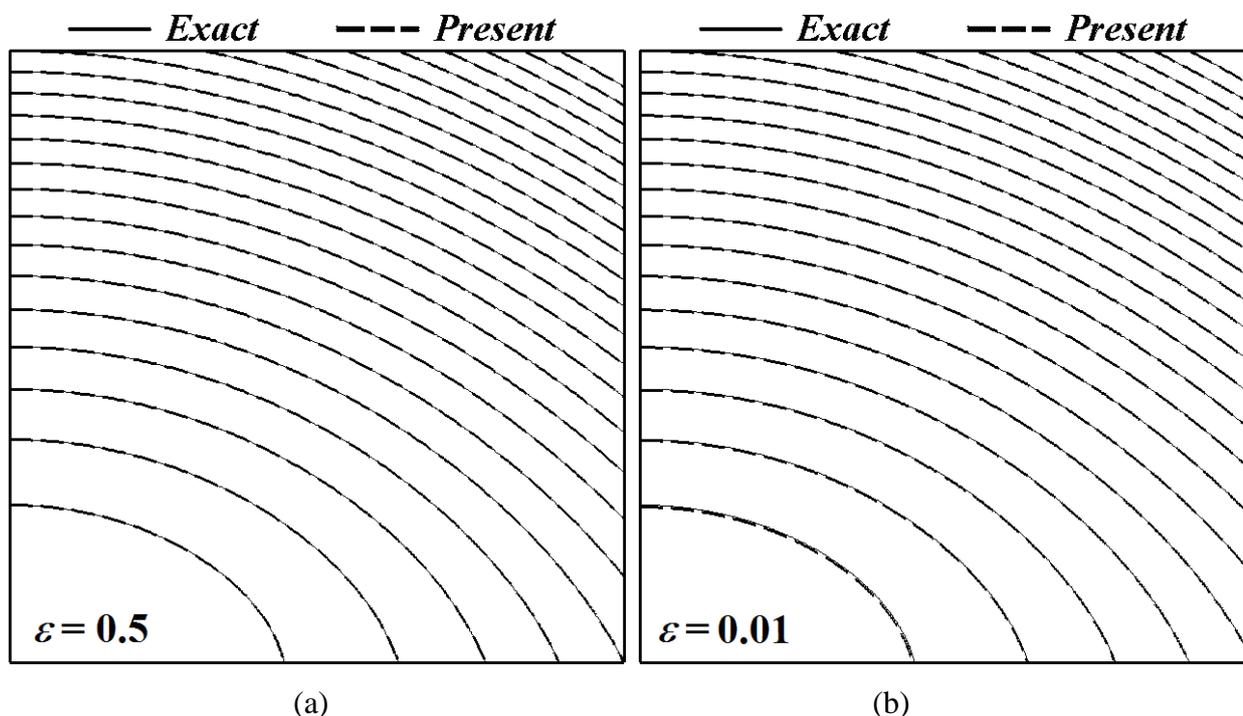
Figure 5: Solutions for diffusion in a medium with a non-linear variable diffusion coefficient with (a) $\varepsilon = 0.50$ and (b) $\varepsilon = 0.01$.
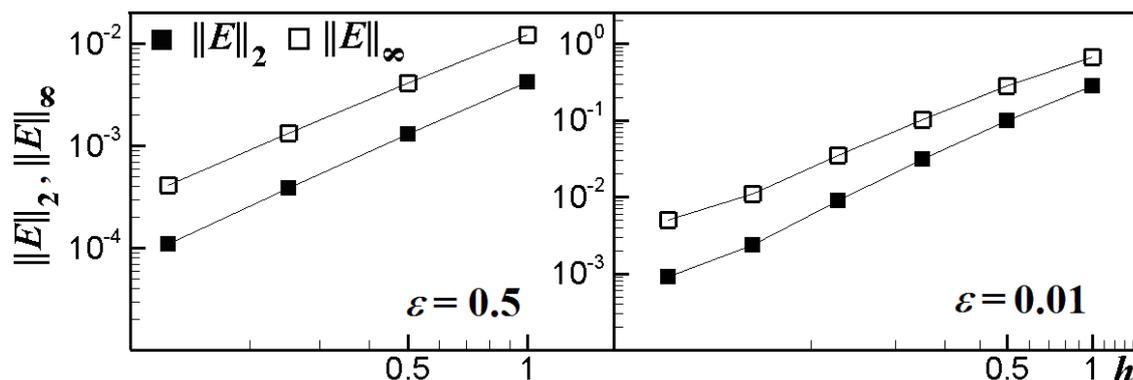
Figure 6: Errors for the case of diffusion in a medium with a non-linear variable diffusion coefficient.

5.3 Diffusion in a heterogeneous anisotropic medium with an asymmetric non-linear variable diffusion coefficient

Asymmetric diffusion coefficient can occur physically, e.g. the electron heat conductivity tensor used in plasma physics [41-42]. The ability to handle asymmetric diffusion tensors is therefore of interest. This exercise concerns diffusion in a unit square with an asymmetric non-linear diffusion coefficient of the form

$$\overline{\overline{\Gamma}} = \begin{bmatrix} 1+x+y & -x^2 \\ y & 1+2x+y \end{bmatrix} \tag{31}$$

The medium has a non-zero variable source term of the form

$$S = 16(1+x+y)\cos 4x + 9(1+2x+y)\sin 3y - 3\cos 3y + 8\sin 4x + 6x\cos 3y \tag{32}$$

At the boundary of the domain, the following mixed boundary condition is enforced.

$$q_n^P(x,0) = 3(1+2x), \quad 0 \le x \le 1 \tag{33a}$$

$$q_n^P(x,1) = -6(1+x)\cos 3 + 4\sin 4x, \quad 0 \le x \le 1 \tag{33b}$$

$$\phi^P(0,y) = 1+\sin 3y, \quad 0 \le y \le 1 \tag{33c}$$

$$\phi^P(1,y) = \cos 4 + \sin 3y, \quad 0 \le y \le 1 \tag{33d}$$

The exact solution for this diffusion process is given by

$$\phi = \cos 4x + \sin 3y \tag{34}$$

Figure 7 shows the mesh independent solution computed on a mesh of 50×50 CVs and the exact solution. A finer mesh is required in this case to sufficiently resolve most features of the solution. The present solution agrees reasonably well with the exact solution. Show in Fig. 8 is the plots of $\|E\|_\infty$ and $\|E\|_2$ against h. This approach retains a comfortable order of accuracy of 1.4966 even in the event of an asymmetric diffusion coefficient in this case. Figure 9 shows the reduction of $\|e\|_\infty$ and $\|E\|_\infty$ during the iterative solution process for both the present and the original formulation on a mesh of 50×50 CVs. The original formulation entails directly solving Eq. (3) via the same iterative procedure as discussed in Section 4.4. Of course without introducing the deferred correction, the original formulation converges within fewer number of iterations. This is generally true for other cases considered here in this article. Therefore, having relatively more iteration to achieve convergence is the price to pay of using the present formulation which allow easy adaption of existing solvers for isotropic diffusion problem to anisotropic diffusion problem by adding a

15

departure from isotropic term implemented in a deferred correction approach. An additional computation is also made where the Dirichlet boundary condition is applied. Visually indistinguishable solution is obtained and therefore is not shown here.
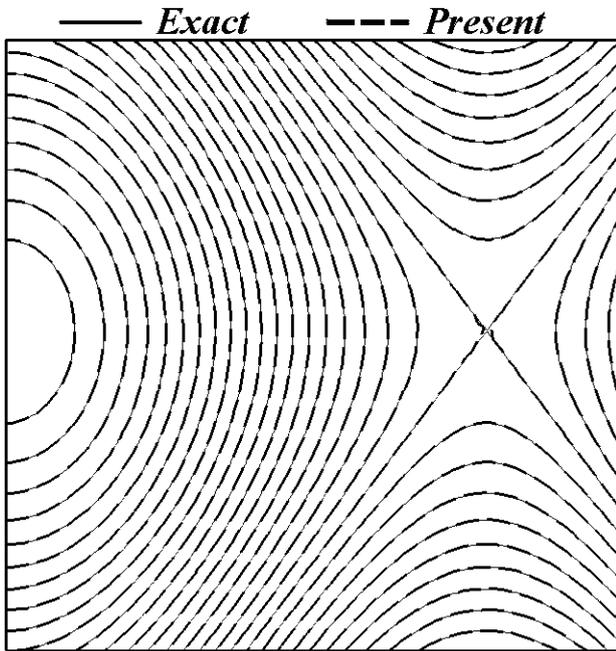

Figure 7: Solution for diffusion in a medium with an asymmetric non-linear variable diffusion coefficient.
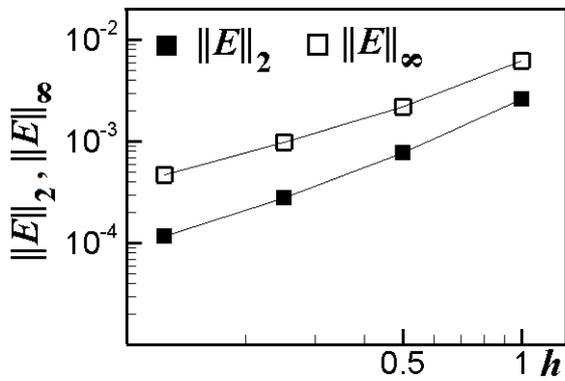

Figure 8: Errors for the case of diffusion in a medium with an asymmetric non-linear variable diffusion coefficient.
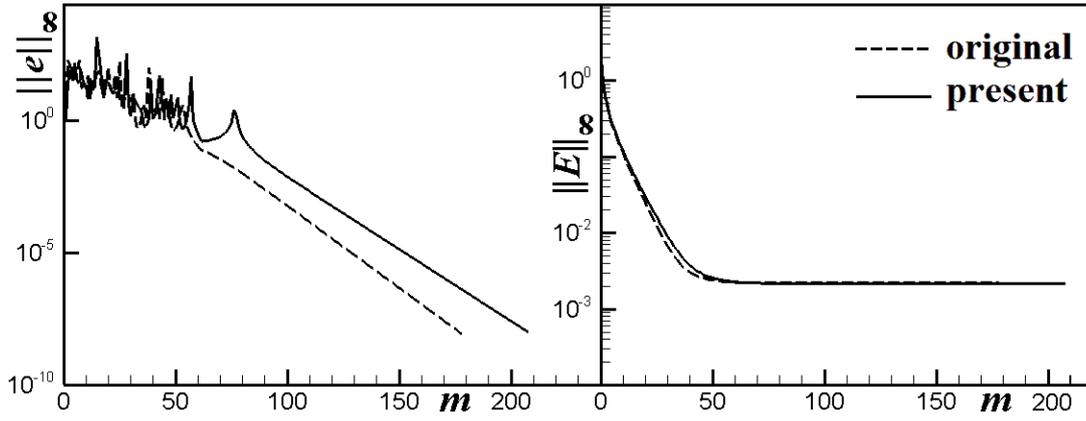
Figure 9: Reduction of $\|e\|_\infty$ and $\|E\|_\infty$ during the iterative solution process for both the present and the original formulation.

5.4 Diffusion in an anisotropic medium with discontinuous diffusion coefficient

The present approach is now applied to an anisotropic medium in which the diffusion coefficient is discontinuous across an irregular internal interface. Here, irregular interface refers to an interface that cannot be represented exactly on a computational mesh, e.g. a Cartesian mesh in the current problem. Figure 10 depicts a domain consisting of two different homogeneous sub-domains defined respectively by $0 \leq rx + sy < \delta$ and $\delta \leq rx + sy \leq 1$. The diffusion coefficient in each sub-domain is constant. It is however discontinuous across the interface between the two sub-domains defined by $rx + sy = \delta$. The diffusion coefficient is given by

$$
\overline{\overline{\Gamma}} = \begin{cases} \begin{bmatrix} 1 & 1/10 \\ 1/10 & 1 \end{bmatrix} & ,0 \leq rx + sy < \delta \\ \begin{bmatrix} 1 & 1/10 \\ 1/10 & 1 \end{bmatrix} \lambda & ,\delta \leq rx + sy \leq 1 \end{cases} \tag{35}
$$

where $0 \leq r,s,\delta \leq 1$ and $r + s = 1$. The diffusion coefficient in the sub-domain of $\delta \leq rx + sy \leq 1$ is λ times larger than that of the sub-domain of $0 \leq rx + sy < \delta$. Note that the directions of both the major and minor principle diffusion coefficients are identical in the two sub-domains. The anisotropy in each sub-domain is not high, e.g. the sub-domain of $0 \leq rx + sy < \delta$ has a principal diffusion coefficient of $\overline{\overline{\Gamma^*}} = \begin{bmatrix} 1.1 & 0 \\ 0 & 0.9 \end{bmatrix}$. The case of enforcing given flux on the top and bottom boundaries and given ϕ on the left and right boundaries is considered in [43-44]. Under such boundary conditions, the exact solution is given by

$$
\phi = \begin{cases} \dfrac{\lambda(rx + sy)}{1 + \delta(\lambda - 1)} & ,0 \leq rx + sy < \delta \\ \dfrac{(rx + sy) + \delta(\lambda - 1)}{1 + \delta(\lambda - 1)} & ,\delta \leq rx + sy \leq 1 \end{cases} \tag{36}
$$

As for boundary conditions, a mixed boundary condition is enforced. Prescribed $\phi^P(0, y)$ and $\phi^P(1, y)$ are enforced respectively at the left and right boundaries. These are evaluated from Eq. (36). Prescribed flux of $q_n^P(x,0)$ and $q_n^P(x,1)$ are imposed at the lower and upper boundaries respectively. $q_n^P(x,0)$ and $q_n^P(x,1)$ can be constructed from Eq. (36) using Eq. (4b). The case of $r = 2/3$, $s = 1/3$, $\delta = 1/3$ and $\lambda = 10$ is considered here. Mesh independent solution, obtained on a mesh of 50×50 CVs, is shown in Fig. 11 together with the exact solution. The present solution is in good agreement with the exact solution. The effect of the discontinuity in the diffusion coefficient is clearly evident in the solution with a much stepper gradient of ϕ in the sub-domain of $0 \le rx + sy < \delta$ where the diffusion coefficient is much smaller. Errors as the mesh is refined are plotted in Fig. 12. The Cartesian mesh employed cannot represent the discontinuity of the diffusion coefficient exactly. More accurate solution can only be obtained by refining the mesh. Therefore it is not surprising that the order of accuracy decreases substantially to 1.1157.
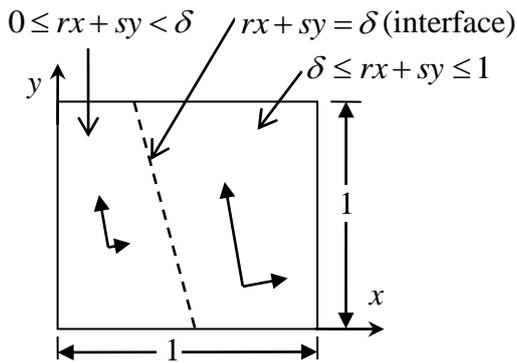
Figure 10: Schematic of an anisotropic medium with discontinuous diffusion coefficient.
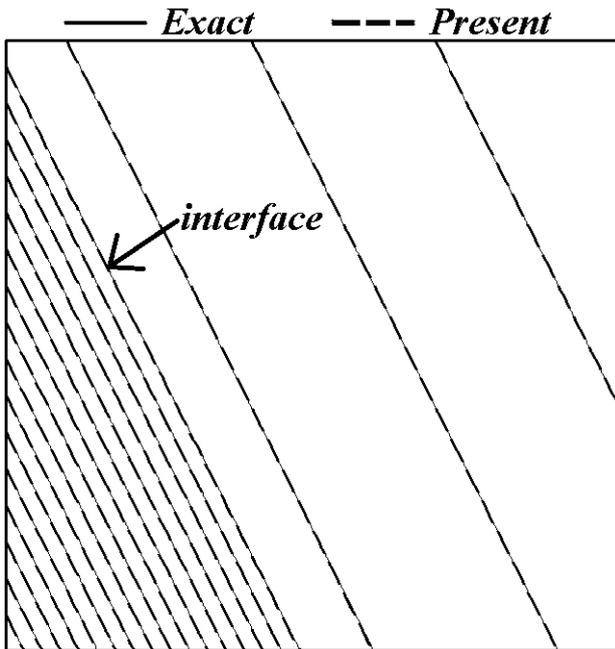
Figure 11: Solution for diffusion in a medium with discontinuous diffusion coefficient.
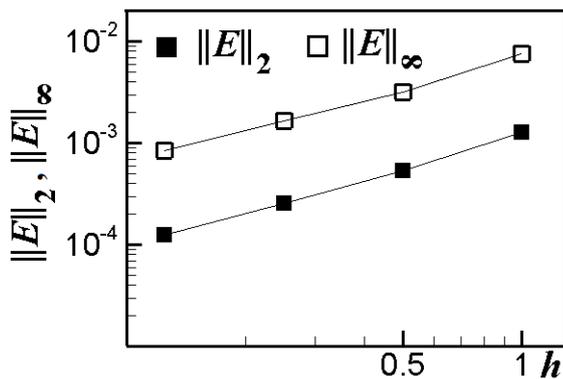
Figure 12: Errors for the case of diffusion in a medium with discontinuous diffusion coefficient.

5.5 Diffusion in an orthotropic medium with discontinuous diffusion coefficient

Figure 13 shows an orthotropic physical domain with a smaller computational domain Ω embedded. The physical domain consists of two sub-domains labelled respectively as l (left, $x^* < 0.5$) and r (right, $x^* \geq 0.5$). The diffusion coefficient is given by

$$\overline{\overline{\Gamma}}^* = \begin{cases} \begin{bmatrix} 50 & 0 \\ 0 & 1 \end{bmatrix} & ,x^* < 0.5 \\ \begin{bmatrix} 1 & 0 \\ 0 & 10 \end{bmatrix} & ,x^* \geq 0.5 \end{cases} \tag{37}$$

There is a discontinuity in the diffusion coefficient across $x^* = 0.5$. The major principle diffusion coefficients in these sub-domains are oriented 90° to each other. Within the domain, there is no source/sink term, i.e. $S = 0$. For such a system, the exact solution can be expressed as [44-45]

$$\phi(x*, y*) = \begin{cases} c_l x*^2 + d_l y*^2 & , x* < 0.5 \\ a_r + b_r x* + c_r x*^2 + d_r y*^2 & , x* \geq 0.5 \end{cases} \tag{38a}$$

where

$$\alpha = \frac{\Gamma^*_{xx,r}}{\Gamma^*_{xx,l}}, \ \beta = \frac{\Gamma^*_{yy,l}}{\Gamma^*_{yy,r}}, \ f = \frac{4a_r}{(\alpha-2)\beta+1} \tag{38b}$$

$$a_r = 1, \ b_r = (\beta-1)f, \ c_r = f, \ d_r = -c_r \frac{\Gamma^*_{xx,r}}{\Gamma^*_{yy,r}} \tag{38c}$$

$$c_l = \alpha\beta c_r, \ d_l = d_r \tag{38d}$$

Solution is sought for the computational domain of $\Omega = (0,1)^2$ oriented with an angle θ from the physical domain. With such an orientation, the discontinuity in the diffusion coefficient generally does not align with the boundary of the Cartesian mesh in Ω. The coordinate system and the diffusion coefficient in Ω are related to those of the physical domain via

$$\vec{x} = R\vec{x}* \tag{39}$$

$$\overline{\overline{\Gamma}}(\vec{x}) = R^T \overline{\overline{\Gamma}}*(\vec{x}*)R \tag{40}$$

where the rotational matrix R is given by

$$R = \begin{bmatrix} \cos\theta & -\sin\theta \\ \sin\theta & \cos\theta \end{bmatrix} \tag{41}$$

At the boundary of the computational domain, prescribed ϕ^P derived from Eq. (38) is enforced. Figure 14 shows the present mesh independent solutions obtained on a mesh of 100×100 CVs for $\theta = 0$ and 30°. For the case of $\theta = 0^o$, the discontinuity in the diffusion coefficient is captured exactly by the boundary of the Cartesian CVs. This is no longer the case for $\theta = 30^o$. The effect of the discontinuity in the diffusion coefficient across the interface is captured reasonable well by the present solution although a much finer mesh is required. These solutions are in good agreement with the exact solution of Eq. (38). From Fig. 15, it can be estimated that the order of accuracy for the case of $\theta = 0^o$ and $\theta = 30^o$ are respectively 1.1825 and 0.8989.
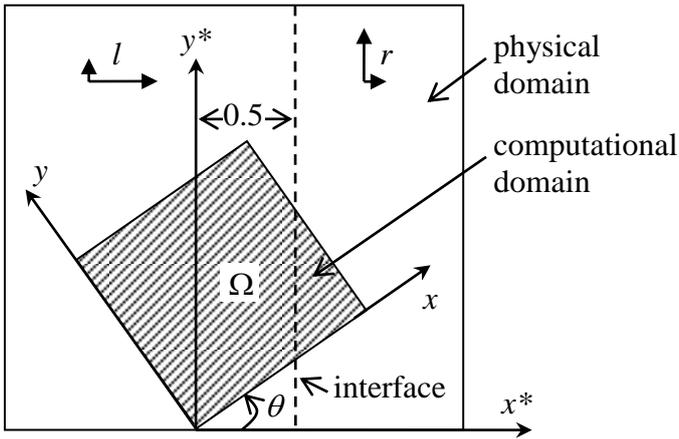
Figure 13: Schematic of an orthotropic medium with discontinuous diffusion coefficient.
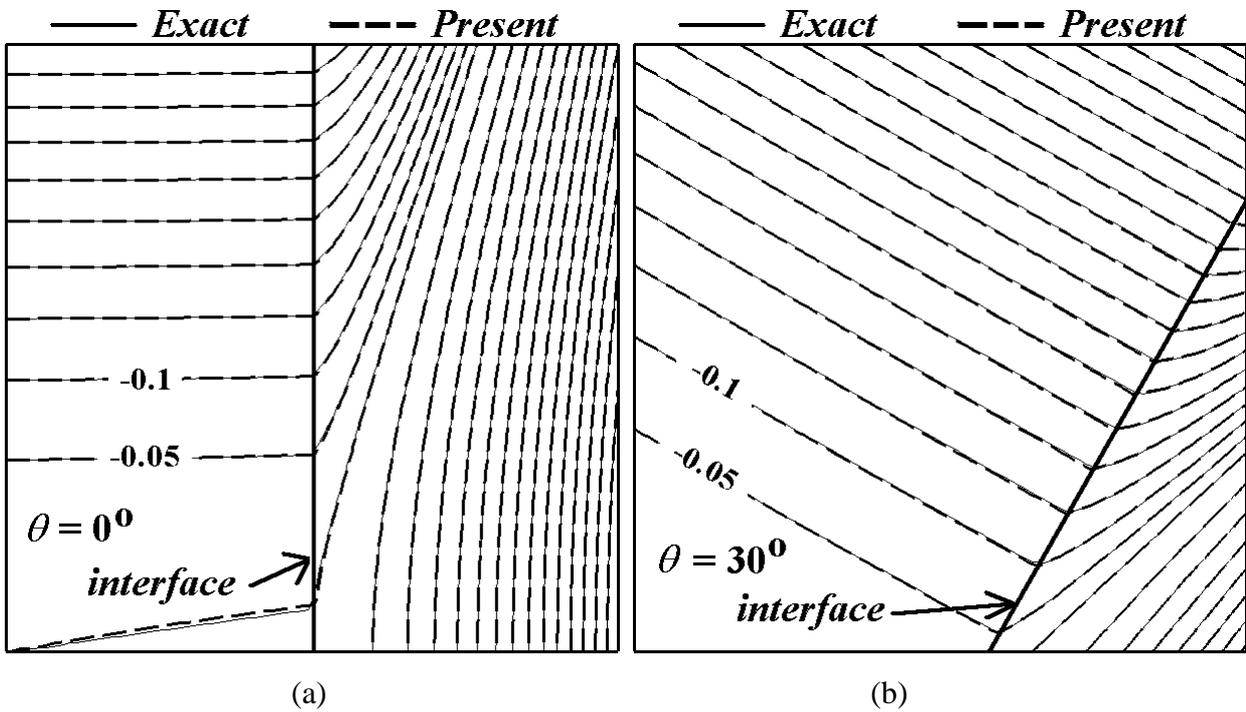
Figure 14: Solutions for diffusion in an orthotropic medium with (a) $\theta = 0^o$ and (b) $\theta = 30^o$.
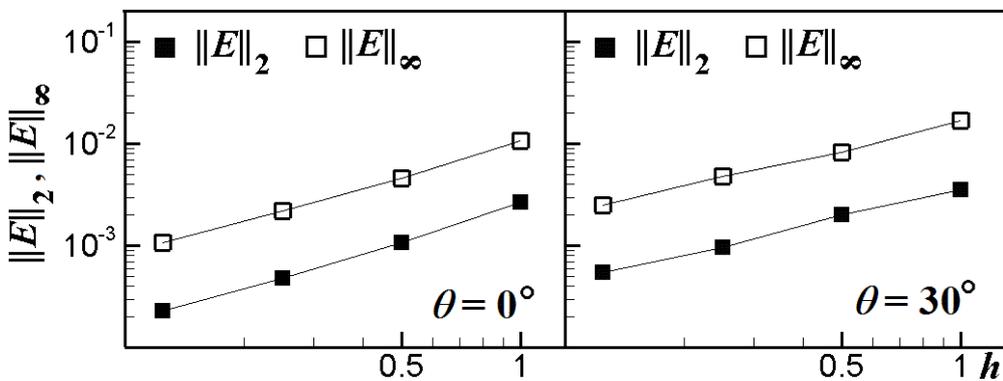
Figure 15: Errors for the case of diffusion in an orthotropic medium with discontinuous diffusion coefficient.

5.6 Heat Conduction in an Anisotropic Medium

Heat conduction in the anisotropic medium with an internal heat source is considered. Figure 16 depicts the domain of interest. Within the hatched region, there is a volumetric heat source of

$$Q_{gen} = 10^5 \cosh(0.84851 x_c) \exp(0.20579 x_c + y_c) \tag{42a}$$

where

$$x_c = (x - 0.2)/0.8 \tag{42b}$$

$$y_c = (y - 0.4)/0.8 \tag{42c}$$

The domain is characterized by the principal conductivity coefficients of $k_{xx}^* = 6.5$ and $k_{yy}^* = 11.3$.

The principal axis of k_{xx}^* is orientated 60° to the x-axis. Based on these, the tensorial conductivity coefficient in the (x, y) coordinate system can be calculated using Eq. (40). As for boundary conditions, the temperatures at the bottom and top of the domain are fixed respectively at $T = 0\,^o\mathrm{C}$ and $T = 50\,^o\mathrm{C}$. The two side walls are insulated. Solutions were obtained on two different meshes, i.e. $16 \times 32\,\mathrm{CVs}$ and $32 \times 64\,\mathrm{CVs}$. The isotherms of $T/50$ for these solutions are shown in Fig. 17. Note that the plot is rotated 90° for a better presentation given large aspect ratio of the domain. A mesh of $16 \times 32\,\mathrm{CVs}$ is sufficient to resolve the essential features of the solution. As expected, the highest temperature occurs at the center of the region with heat source. Due to the anisotropy of the medium, the solution is not symmetric along $x = 0.2$ and the isotherms are not perpendicular to the physical domain. The temperature along the two insulated side walls at $x = 0$ and $x = 0.4$ can be evaluated using Eq. (2) in a post-processing calculation. These are shown in Fig. 18. Comparison is made against those of the boundary element method and the commercial software ANSYS of which are both presented in [46]. The present solution agrees well with these solutions.
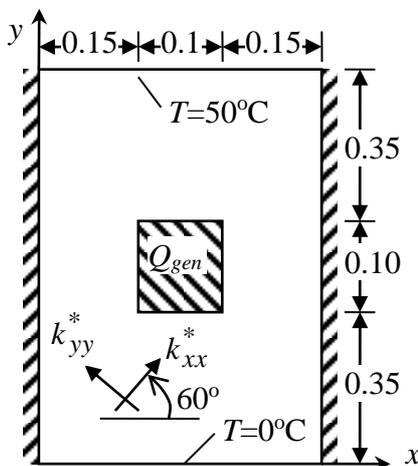

Figure 16: Schematic of an anisotropic medium with an internal heat source.
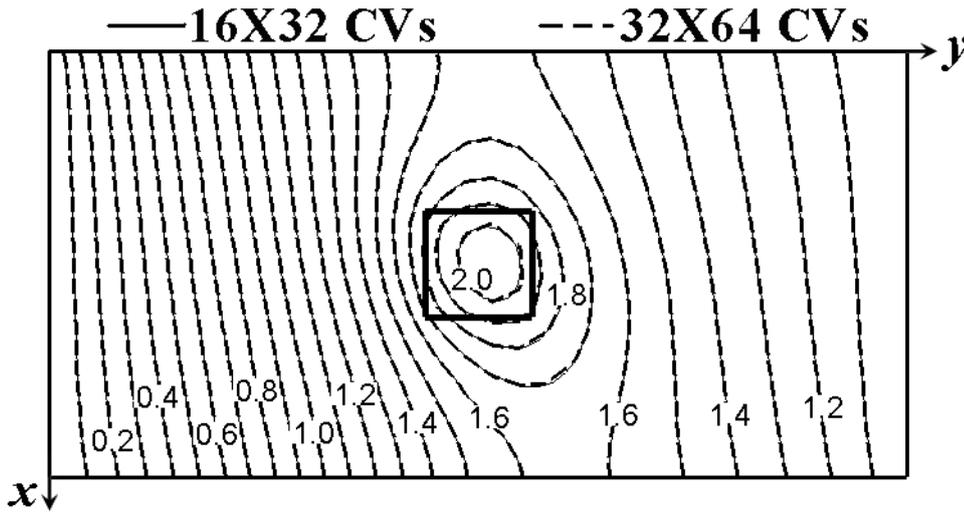
Figure 17: Normalized isotherms for heat conduction in an isotropic medium.
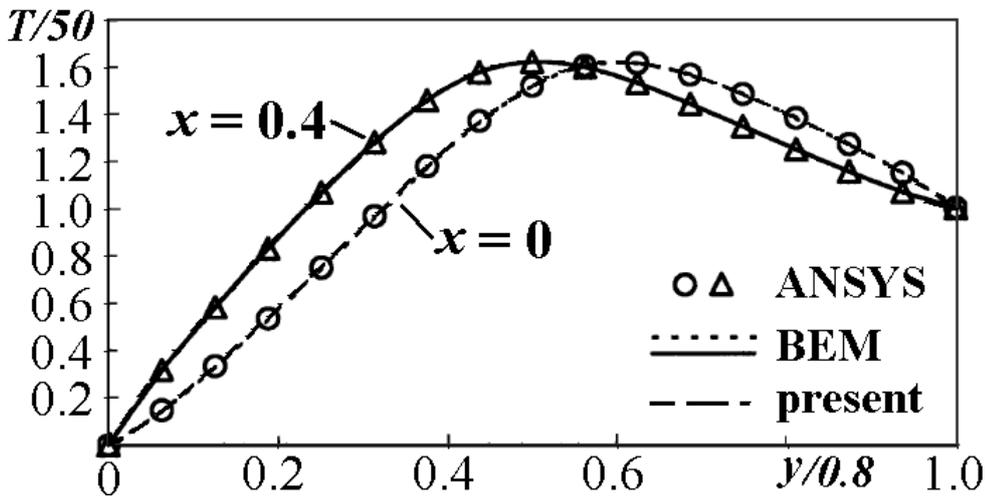

Figure 18: Normalized temperature along the insulated side walls.

5.7 Flow in a multi-layered anisotropic porous medium

Fluid flow through a multi-layered anisotropic porous medium shown in Fig. 19 is considered. The flow is governed by the Darcy's law in the form of Eq. (2) where $\vec{q}$, $\overline{\overline{\Gamma}}$ and ϕ are respectively the velocity vector, permeability tensor and pressure. Coupling this with the continuity equation, an anisotropic diffusion equation of the form of Eq. (1) can be derived for the pressure. The multi-layered porous medium consists of a total of three different homogeneous anisotropic layers labelled as A, B and C. The principal permeability tensors for the layer A, B and C are respectively

$$\overline{\overline{\Gamma}}_A^* = \begin{bmatrix} 6 & 0 \\ 0 & 1 \end{bmatrix}, \theta_A = 60^o \tag{43a}$$

23

$$\overline{\overline{\Gamma_B^*}} = \begin{bmatrix} 4 & 0 \\ 0 & 1 \end{bmatrix} , \theta_B = 60^o \tag{43b}$$

$$\overline{\overline{\Gamma_C^*}} = \begin{bmatrix} 2 & 0 \\ 0 & 1 \end{bmatrix} , \theta_C = 60^o \tag{43c}$$

The domain is subjected to the following mixed boundary conditions:

$$\phi^P(x,0) = 1, \ \ 0 \le x \le 1 \tag{44a}$$

$$\phi^P(x,2) = 0, \ \ 0 \le x \le 1 \tag{44b}$$

$$q_n^P(0, y) = q_n^P(1, y) = 0, \ \ 0 \le y \le 1 \tag{44c}$$

Note that the right and left boundaries are impermeable. A unit pressure difference is applied across the medium in the y-direction. The computed pressure is presented in the first plot of Fig. 20. Comparison was made against that of Lorinczi et al. [39] where good agreement is attained. The velocity field is shown in the second plot of Fig. 20. Generally, due to the anisotropic nature of the porous medium, the flow direction is strongly dictated by the permeability tensor characterising the medium.
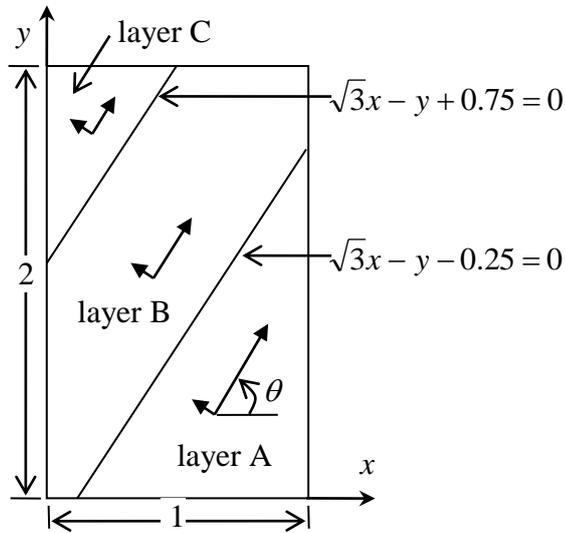
Figure 19: Schematic of a multi-layered anisotropic porous medium.
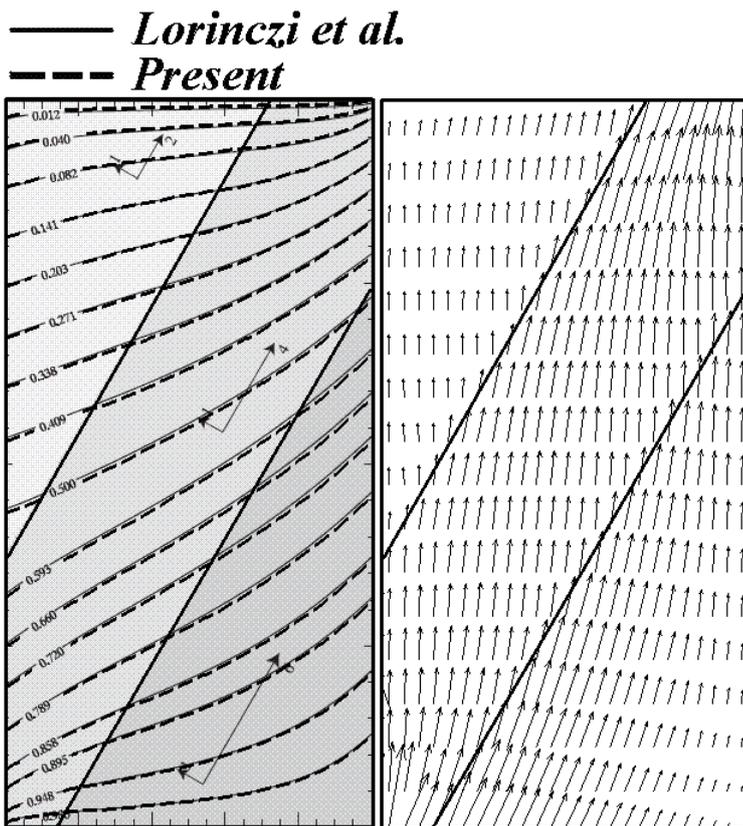
Figure 20: Pressure and velocity field for flow through a multi-layered anisotropic porous medium.

6 Concluding Remarks

This article presents an approach of adapting solvers for *isotropic* diffusion equations to solve *anisotropic* diffusion equations. The formulation works by decomposing the diffusive flux into a component associated with isotropic diffusion and another component associated with departure from isotropic diffusion. This results in an *isotropic* diffusion equation with additional terms to account for the anisotropic effect. These additional terms are treated using a deferred correction approach and coupled via an iterative procedure. Validations of the present approach were performed for diffusion in various anisotropic media. The approach is applied to investigate heat conduction in anisotropic medium with internal heat generation and flow in a multi-layered anisotropic porous medium. Although demonstrated for two-dimensional problems, extension of the present approach to three-dimensional problems is straight forward. In this article, the approach is demonstrated using the finite volume method. It can however be applied equally well for any discretization method including the finite difference and finite element methods.

Acknowledgement

References

1. Fick A.. On liquid diffusion. J Membrane Sci 1995;10:33-38.

2. Hassanizadeh SM. Derivation of basic equations of mass transport in porous media, Part 1: Macroscopic balance laws. Adv Water Resour 1989;9:196-206.

3. Jawitz JW. Solute diffusion in porous media. CWR 6537 Subsurface Contaminant Hydrology, University of Florida, Lecture notes, http://soils.ifas.ufl.edu/hydrology/teaching/csh/ [accessed on 15th Feb 2012]

4. Berkowitz B. Characterizing flow and transport in fractured geological media: a review. Adv Water Resour 2002;25:861–884.

5. Saadatfar M, Sahimi M. Diffusion in disordered media with long-range correlations: anomalous, Fickian, and superdiffusive transport and log-periodic oscillations. Phys Rev B 2002;65:036116.

6. Bear J. Dynamics of Fluids in Porous Media. Dover Publication; 1972.

7. Das B, Steinberg S, Weber S. Finite difference methods for modelling porous media flows. Transport Porous Med 1994;17:171-200.

8. Ozisik MN. Heat Conduction, Second Ed. John Wiley & Sons; 1993.

9. Traiano FML, Cotta RM, Orlande HRB. Improved Approximate Formulations for Anisotropic Heat Conduction. Int Comm Heat Mass Transfer 1997;24:869-878.

10. Abdul Azeez MF and Vakakis AF. Axisymmetric Transient Solutions of the Heat Diffusion Problem in Layered Composite Media. Int J Heat Mass Transfer 2000;43:3883-3895.

11. Basser PJ, Jones DK. Diffusion-tensor MRI: theory, experimental design, and data analysis-a technical review. NMR Biomed 2002;15:456-467.

12. Perona P, Malik J. Scale-space and edge detection using anisotropic diffusion. IEEE Trans Pattern Anal Mach Intel 1990;12:629–639.

13. Weickert J. Anisotropic Diffusion in Image Processing. Teubner-Verlag; 1998.

14. Karras DA, Mertzios GB. New PDE-based methods for image enhancement using SOM and Bayesian inference in various discretization schemes. Meas Sci Technol 2009;20:104012.

15. Thomas JW. Numerical Partial Differential Equations: Finite Difference Methods. Springer-Verlag; 1995.

16. Solin P. Partial Differential Equations and the Finite Element Method. John Wiley & Sons; 2006.

17. Patankar SV. Numerical Heat Transfer and Fluid Flow. Hemisphere Publisher; 1980.

18. Taigbenu AE, Liggett JA. Boundary element calculations of diffusion equation. J Eng Mech 1985;111:311-328.

19. Bernhardt PA, Brackbill JU. Solution of elliptic equations using fast Poisson solvers. J Comput Phys 1984;53:382-394.

20. Breil J, Maire PH. A cell-centered diffusion scheme on two-dimensional unstructured meshes. J Comput Phys 2007;224:785-823.

21. Katayama K, Saito A. Transient Heat Conduction in Anisotropic Solids. Proc. of 5th International Heat Transfer Conference 1974;1: 137-141.

22. Sharma P, Hammett GW. A Fast Semi-implicit Method for Anisotropic Diffusion. J Comput Phys 2011;230:4899-4909.

23. Hyman J, J Morel E, Shashkov M, Steinberg S. Mimetic finite difference methods for diffusion equations. Comput Geosci 2002;6:333–352.

24. Gyrya V, Lipnikov K. High-order mimetic finite difference method for diffusion problems on polygonal meshes. J Comput Phys 2008;227:8841–8854.

25. Murthy JY, Mathur SR. Computation of Anisotropic Conduction Using Unstructured Meshes. J Heat Transfer 1998;120:583-591.

26. Pasdunkorale JA, Turner IW. A second order finite volume technique for simulating transport in anisotropic media. Int J Numer Meth Heat Fluid Flow 2003;13:31-56.

27. Edwards MG, Zheng H. Quasi-positive families of continuous Darcy-flux finite volume schemes on structured and unstructured grids. J Comp Appl Math 2010;234:2152-2161.

28. Aavatsmark I, Barkve T, Boe O, Mannseth T. Discretization on unstructured grids for inhomogeneous, anistropic media, Part I: Derivation of the methods, SIAM J Sci Comput 1998;19:1700-1716.

29. Aavatsmark I, Barkve T, Boe O, Mannseth T. Discretization on unstructured grids for inhomogeneous, anistropic media, Part II: Discussion and numerical results. SIAM J Sci Comput 1998; 19:1717-1736.

30. Edwards MG. M-matrix flux splitting for general full tensor discretization operators on structured and unstructured grids. J Comput Phys 2000;160:1-28.

31. Pal M, Edwards MG. Non-linear flux splitting schemes with imposed discrete maximum principle for elliptic equations with highly anisotropic coefficients. Int J Numer Meth Fluids 2011;66:299-323.

32. Nakshatrala KB, Valocchi A.J. Non-negative mixed finite element formulations for a tensorial diffusion equation. J Comput Phys 2009;228:6726–6752.

33. Kuzmin D, Shashkov MJ, Svyatskiy D. A constrained finite element method satisfying the discrete maximum principle for anisotropic diffusion problems. J Comput Phys 2009;228:3448–3463.

34. Li X, Huang W. An anisotropic mesh adaptation method for the finite element solution of heterogeneous anisotropic diffusion problems. J Comput Phys 2010;229:8072–8094.

35. Shiah YC, Lee RF. Boundary element modeling of 3D anisotropic heat conduction involving arbitrary volume heat source. Math Comput Model 2011;54:2392–2402.

36. Zhang YM, Liu ZY, Chen JT, Gu Y. A novel boundary element approach for solving the anisotropic potential problems. Eng Anal Bound Elem 2011;35:1181–1189.

37. Versteeg HK. Malalasekera W. An Introduction to Computational Fluid Dynamics: The Finite Volume Method, 2nd ed. Prentice Education Limited; 2007.

38. Roache PJ. Code verification by the method of manufactured solution. J Fluids Eng 2002;124:4-10.

39. Lorinczi P, Harris SD, Elliott L. Modified flux-vector-based Green element method for problems in steady-state anisotropic media. Eng Anal Bound Elem 2009;33:368-387.

40. Le Potier C. Finite volume monotone scheme for highly anisotropic diffusion operators on unstructured triangular meshes. Comptes Rendus Mathematique 2005;341:787-792.

41. Braginskii SI. Transport Process in Plasma, Reviews of Plasma Physics, Vol. I. Consultants Bureau; 1965.

42. Maire PH, Breil J. A nominally second-order accurate finite volume cell-centered scheme for anisotropic diffusion on two-dimensional unstructured grids. J Comput Phys 2012;231:2259–2299.

43. Hyman J, Shashkov M, Steinberg S. The Numerical Solution of Diffusion Problems in Strongly Heterogeneous Non-isotropic Materials. J Comput Phys 1997;132:130–148.

44. Edwards MG, Rogers CF. Finite volume discretization with imposed flux continuity for the general tensor pressure equation. Computat Geosci 1998;2:259–290.

45. Friis HA, Edwards MG. A family of MPFA finite-volume schemes with full pressure support for the general tensor pressure equation on cell-centered triangular grids. J Comput Phys 2011;230:205-231.

46. Shiah YC, Lim CY. Anisotropic heat conduction involving internal arbitrary volume heat generation rate. Int Comm Heat Mass Transfer 2002;29:1079-1088.

Nomenclature

A	surface area of a control volume
$\|E\|_2$	root mean square norm error
$\|E\|_\infty$	maximum norm of error
h	refinement ratio
$\bar{\bar{I}}$	identity matrix
k	thermal conductivity
$\vec{q}$	diffusive flux
$\vec{q}_D$	departure from isotropic component of the diffusive flux
$\vec{q}_{max}$	isotropic component of the diffusive flux
Q_{gen}	volumetric heat generation
R	rotational matrix
S	source term
S_D	source term due to departure from isotropic
T	temperature
$\vec{x}$	position vector
x	coordinate axis
y	coordinate axis

Greek letters

ΔV	volume
ΔA	surface area
ε	degree of anisotropic
ϕ	transported quantity
$\bar{\bar{\Gamma}}$	diffusion coefficient
Γ_{max}	isotropic component of the diffusion coefficient
$\bar{\bar{\Gamma}}_D$	departure from isotropic component of the diffusion coefficient
Ω	domain of interest
$\partial\Omega^q$	boundary with prescribed flux
$\partial\Omega^\phi$	boundary with prescribed ϕ
θ	orientation of the principal directions

Superscript

m current iteration

P prescribed value

*   principal directions

Subscript

ave   average

B boundary control volume

n normal

P control volume P

List of Figures